Journal of Power Sources 249 (2014) 9–12

Contents lists available at ScienceDirect

Journal of Power Sources

journal homepage: www.elsevier.com/locate/jpowsour

Short communication

Ethylene glycol electrooxidation on core–shell PdCuBi nanoparticles fabricated via substitution and self-adsorption processes

Yiyin Huang [a], Yonglang Guo [b], Yaobing Wang [a,*]

[a] State Key Laboratory of Structural Chemistry, Fujian Institute of Research on the Structure of Matter, Chinese Academy of Sciences, YangQiao West Road 155#, Fuzhou 350002, PR China
[b] College of Chemistry and Chemical Engineering, Fuzhou University, Fuzhou 350108, PR China

HIGHLIGHTS

- PdCuBi particles were fabricated via substitution and self-adsorption processes.
- The particles possess the virtues of core–shell structure and surface modification.
- Peak current on PdCuBi/C for EG oxidation was three times higher than that on Pd/C.
- Catalytic durability of PdCuBi/C for EG oxidation was greatly improved.

GRAPHICAL ABSTRACT

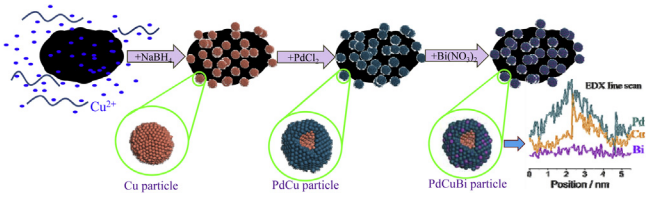

ARTICLE INFO

Article history:
Received 26 August 2013
Received in revised form
16 October 2013
Accepted 17 October 2013
Available online 25 October 2013

Keywords:
Alkaline medium
Core–shell structure
Ethylene glycol oxidation
Palladium

ABSTRACT

Partial substitution of Cu by Pd^{2+} ions and Bi^{3+} ion self-adsorption processes are used to fabricate a novel core–shell PdCuBi nanocatalyst. X-ray diffraction, transmission electron microscope, energy-dispersive X-ray spectra and different electrochemical measurements are used to characterize the catalyst. It is exhibited that Pd covers Cu outer layers in the substitution reaction and Bi modifies Pd surface in the adsorption process. The peak current for ethylene glycol electrooxidation of PdCuBi/C (171.1 mA cm^{-2}) in a KOH solution is almost three times higher than that of Pd/C (57.8 mA cm^{-2}). Durability and tolerance towards strongly adsorbed intermediate poisoning of this catalyst are also improved.

1. Introduction

As an appealing candidate for fuel cell applications, ethylene glycol has attracted much attention because of its low toxicity, low membrane penetration, while high boiling point and high energy density [1,2]. At room temperature, ethylene glycol is hard to be completely oxidized to CO_2 owing to the difficulty of C–C bond dissociation [3,4]. However, the research on the electrochemical kinetics and reaction mechanism shows that the electrooxidation reaction of ethylene glycol displays high activity in alkaline medium [5]; and the recent development in alkaline solid membrane electrolyte gives a great potential of using ethylene glycol as a fuel in alkaline fuel cells.

Pd has certain catalytic effects on alcohol electrooxidation in alkaline medium [6,7]. Besides, Pd is much more abundant compared to Pt on the earth [8] and thus the Pd-based catalysts have an advantage in cost, which facilitates their commercialization application. However, the activity of Pd-based catalysts should be further enhanced as they are used in practical fuel cells. For this purpose, uniform nanocatalysts with large surface area

* Corresponding author. Tel./fax: +86 591 2285 3916.
E-mail address: wangyb@fjirsm.ac.cn (Y. Wang).

0378-7753/$ – see front matter © 2013 Elsevier B.V. All rights reserved.
http://dx.doi.org/10.1016/j.jpowsour.2013.10.083

and high activity per unit area are needed to design; and various approaches were proposed to achieve these conditions, such as size control [9], surface modification [10], shape selection [11], and fabrication of hollow or core–shell nanoparticles [12,13]. So far, most of previous research focused on the single factor; while the joint action of two or more factors above can greatly improve catalytic activity. For example, modification with other active metals on core–shell particle surfaces is a feasible approach to obtain highly active catalysts. Recently, it is reported that Bi [14] and Cu [15,16] had some promoting effects on the catalyst for electrooxidation of small organic molecules. Bi^{3+} ions can modify Pd surface by spontaneous and irreversible deposition processes [14,17], which is so-called Bi ion self-adsorption. In addition, Cu can be easily substituted by noble metal ions [18]. In this work, a simple and efficient route to prepare core–shell PdCuBi nanoparticles on active carbon support by a substitution reaction and a self-adsorption process is demonstrated. The electrocatalytic performance of PdCuBi/C towards ethylene glycol oxidation was investigated, compared with Pd/C and PdCu/C.

2. Experimental

2.1. Synthesis of catalysts

Active carbon (Vulcan XC-72R) was first pretreated with concentrated HNO_3 at 120 °C for 1 h. Then, the mixture was neutralized with NaOH, filtered, washed with double distilled water and dried overnight. The PdCuBi/C catalyst was prepared as follows: 90 mg of pretreated Vulcan XC-72R carbon and 118 mg of $CuSO_4 \cdot 5H_2O$ were dispersed in a mixture of water/ethylene glycol (1/1, volume ratio) under stirring. An excess $NaBH_4$ solution was added to reduce Cu^{2+} ions to Cu particles and the reduction reaction was conducted for 1 h. This mixture was then filtered, washed and dried to obtain Cu/C composite. 122.5 mg of Cu/C was dispersed in 50 ml of double distilled water, and 3.4 ml of 37.8 mM H_2PdCl_4 aqueous solution was added slowly into the suspension under vigorous stirring. The galvanic substitution reaction of Pd^{2+} ions to Pd by oxidizing Cu was conducted for 1 h. Afterward, 0.32 ml of 18.9 mM $Bi(NO_3)_3$ was added very slowly into the solution and the adsorption reaction was sustained for 2 h. Finally, the mixture was filtered, washed and dried overnight. The PdCu/C and Pd/C catalysts were synthesized via the same method.

2.2. Physical and electrochemical characterization

The X-ray diffraction (XRD) patterns of the catalysts were performed using a Philip X'Pert Pro MPP X-ray powder diffractometer with Cu K_α radiation ($\lambda = 1.5418$ Å) at a scan rate of 2° min^{-1} with a step of 0.02°. The morphology and energy-dispersive X-ray (EDX) analysis of the catalyst were characterized using a JEOL JEM-2010 transmission electron microscope (TEM) with a microanalyser whose resolution power is 129 eV.

The electrochemical measurements of the catalysts were performed using a CHI660C electrochemical working station (CH Instrument Inc.). The mercuric oxide electrode (Hg/HgO/1 M KOH, 0.098 V *vs.* SHE [19]) and the mercury sulfate electrode (Hg/Hg_2SO_4/0.1 M H_2SO_4, 0.615 V *vs.* SHE [20]) were used as the reference electrodes. A Pt foil was used as the counter electrode. A piece of glassy carbon (0.1256 cm^2) covered by the catalyst was used as the working electrode. For the working electrode preparation, a specific amount of the catalyst was dispersed in a suspension of 15 μl of 15 wt% Nafion solution (DuPont, USA) and 985 μl isopropyl alcohol under ultrasonic stirring. An aliquot of the slurry was spread on the polished glassy carbon electrode surface and the electrode was dried at 80 °C for 30 min. The total Pd loading on the electrode kept 4 μg. All solutions were first de-aerated with high purity N_2 before measurements.

3. Results and discussion

The compositions of the as-prepared catalysts were analyzed by EDX spectra. The practical Pd loadings in PdCuBi/C, PdCu/C and Pd/C catalysts are 9.69 wt%, 10.38 wt% and 20.7 wt%, respectively. The atomic ratios of Pd:Cu:Bi and Pd:Cu in PdCuBi/C and PdCu/C are 1:1.23:0.02 and 1:1.09, respectively. The Cu content is lower than its initial additive amount probably because partial Cu was oxidized before Pd^{2+} ion substitution and then the Cu oxide suffered dissolution in the acid solution during substitution; besides, partial substitution of Cu by Pd^{2+} also results in a decrease of Cu content in the catalysts. The Bi content is too low to be determined accurately, however, most of Bi can be adsorbed on Pd surface within 2 h [14].

The XRD patterns of PdCuBi/C, PdCu/C and Pd/C catalysts are shown in Fig. 1. The diffraction peak at 24.9° is corresponding to the (0 0 2) plane of hexagonal structure of Vulcan XC-72 carbon support. The four peaks of Pd/C at 39.9°, 45.9°, 67.4° and 80.8° are assigned to Pd (1 1 1), (2 0 0), (2 2 0) and (3 1 1) planes of the Pd *fcc* crystal (JCPDS-ICDD, Card No. 46-1043), respectively. After the substitution reaction, the alloying between Pd and Cu is confirmed by the formation of PdCu (1 1 1) peak at 40.9° (JCPDS-ICDD, Card No. 48-1551). The molar fraction and the alloying degree of Cu in PdCu/C, determined from Vegard's law [21,22], are 0.237 and 28.5%, respectively. This result indicates that part of Cu was not alloyed with Pd and it may exist as thin and/or amorphous phases on the catalyst surface because the relevant peaks are not observed in the PdCu/C pattern. Bi can aggregate on the Pd particle surfaces via the spontaneous chemisorption process after its addition [14]. The deposited Bi may disperse as atoms on Pd particle surfaces because its content is very low compared to Pd; and this dispersion is too thin to be observed in XRD analysis in Fig. 1.

The morphology and particle size distribution of the as-prepared PdCuBi/C catalyst are displayed in Fig. 2A, B and C. As shown in Fig. 2A, most of the metal nanoparticles are uniformly dispersed on the carbon surface. Electronic diffraction (ED) pattern (inset in Fig. 2A) shows an obvious ring corresponding to the PdCu (1 1 1) lattice plane, proving that Pd was alloyed with Cu in the catalyst. Based on the statistics of 360 particles, the average

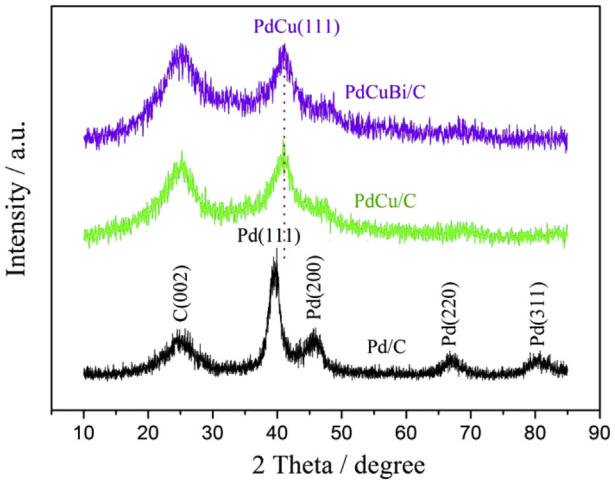

Fig. 1. XRD patterns of PdCuBi/C, PdCu/C and Pd/C.

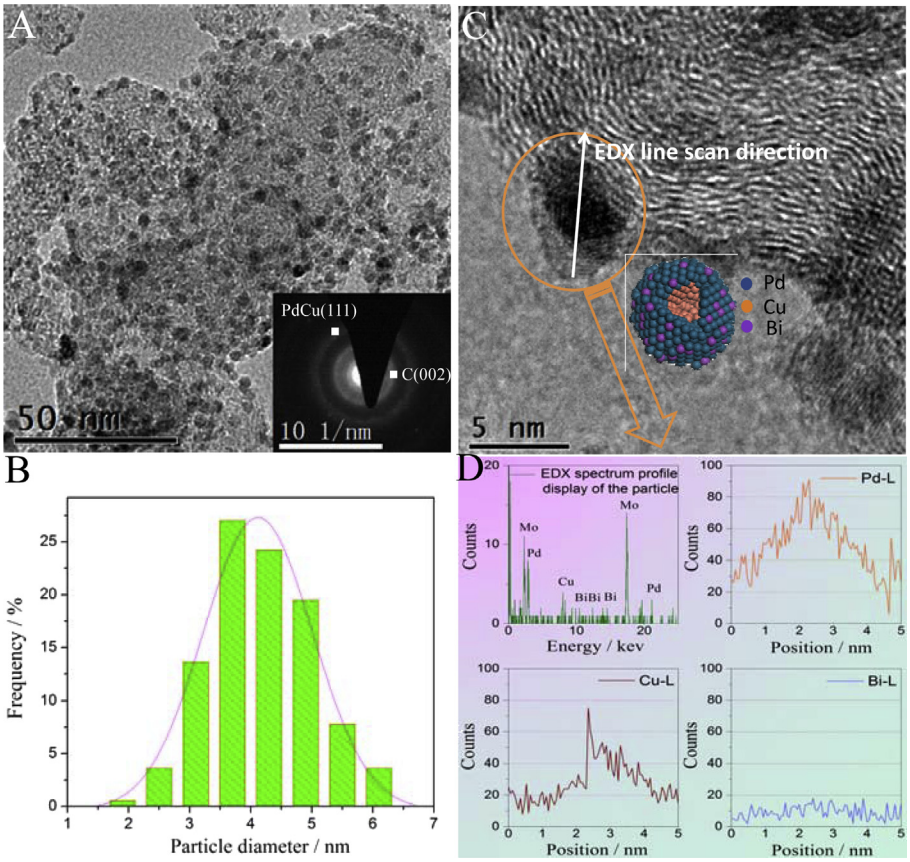

Fig. 2. (A) The low-magnification TEM image of PdCuBi/C and (B) the corresponding particle size distribution; (C) the high-magnification TEM image of PdCuBi/C; (D) EDX line scan of a typical PdCuBi particle.

diameter of these metal nanoparticles is ca. 4.2 nm in Fig. 3B. The high-magnification TEM image shows a typical PdCuBi nanoparticle, and the EDX pattern confirms the particle's trimetallic nature (Fig. 2D). The EDX line scan was conducted to analyze the structure of the PdCuBi nanoparticle and the scanning direction is depicted as the white arrow line. During scanning across the particle, the Pd content rises quickly from the beginning, while the Cu content rises steeply at about 2.2 nm. This phenomenon is characteristic of a Cu@Pd core–shell nanoparticle. The Bi distribution across the particle keeps low and uniform, indicating its low content and the adsorbed layers are very thin.

The electrochemical measurement data are shown in Fig. 3. The coulombic charge (Q) for PdO reduction after deducting corresponding background in the inset in Fig. 3A is 559, 705 and 670 μC for PdCuBi/C, PdCu/C and Pd/C, respectively. The electrochemical surface area (ECSA) of Pd derived from Q [23] is 33.0, 41.6 and 39.5 $m^2\ g^{-1}$ for PdCuBi/C, PdCu/C and Pd/C, respectively. This result suggests that Pd aggregates on the outer shells of the particles and Bi occupies part of Pd active sites. The anodic currents for the dissolution of Cu from the lattice are not observed in the KOH and H_2SO_4 solution, suggesting that Cu was located inside the particles and Pd atoms wrapped the particles. The Cu inside the particles may change the adsorption properties of outer noble metal atoms towards small molecules [24,25], thus enhancing the catalytic activity of the catalyst. There are two clear oxidation peaks at around −0.05 V on the PdCu/C and PdCuBi/C catalysts in Fig. 3A, which is crucial to electrocatalytic oxidation of small organic molecules because it facilitates removal of strongly adsorbed intermediates via a bifunctional mechanism [26]. Ethylene glycol electrooxidation on the as-prepared catalysts is shown in Fig. 3B. The oxidation peak currents of PdCuBi/C, PdCu/C and Pd/C catalysts are 171.1, 105.2 and 57.8 mA cm^{-2}, respectively. Compare these values with the ECSA above, it can be deduced that the enhancement in inherent catalytic activity (depending on the kinetics of the reaction) is the main reason for the increased peak currents of Pd/C after Cu and Bi addition. The constant potential tests in the 1 M KOH + 0.5 M $(CH_2OH)_2$ solution were used to further evaluate durability and tolerance towards strongly adsorbed intermediate poisoning of the as-prepared catalysts as shown in Fig. 3C. Note that both accumulation of poisoning intermediates on catalyst surface and dissolution of metal components can result in a decrease of current. CV after constant potential tests was conducted to distinguish these factors. It is found the peak currents in the stable CVs (inset in Fig. 3C) are very close to those in Fig. 3B, respectively. Consider that dissolution of metal components normally causes an unrecoverable activity loss; the main reason for the decrease of currents in constant potential tests is probably not dissolution of metal but accumulation of poisoning intermediates. PdCuBi/C catalyst has the highest initial and final currents among the three catalysts, expressing its best catalytic durability towards ethylene glycol oxidation. The anti-poisoning ability of the catalysts was further evaluated by linear current sweep curves in Fig. 3D. It is obvious that the PdCuBi/C catalyst has the lowest apparent steady potential platform and the longest polarization time of 613 s at the point of steep hop in potential. This result can be attributed to faster dehydrogenation and easier removal of strongly adsorbed intermediates on Bi-modified core–shell PdCu particle surfaces during ethylene glycol electrooxidation [27].

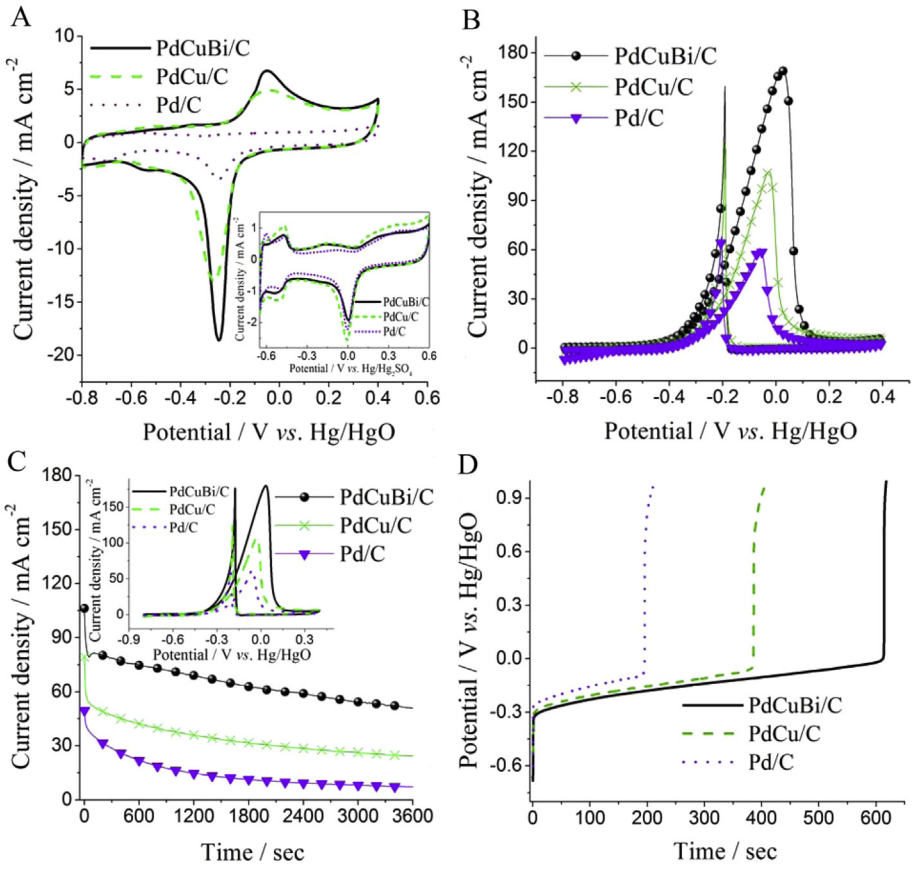

Fig. 3. Cyclic voltammograms of the as-prepared catalysts in (A) 1 M KOH, (inset in A) 0.5 M H_2SO_4 and (B) 1 M KOH + 0.5 M $(CH_2OH)_2$. Scan rate: 50 mV s^{-1}. (C) Current–time curves at −0.1 V, (inset in C) CVs after constant potential tests and (D) linear current sweep at 0.16 mA cm^{-2} s^{-1} of the as-prepared catalysts in 1 M KOH + 0.5 M $(CH_2OH)_2$.

4. Conclusions

The novel fabricated PdCuBi/C catalyst in this study possessed the advantages of both a core–shell structure and surface modification. PdCu nanoparticles with Pd-rich outer layers had more active sites compared to Pd/C. The additional Cu and self-adsorbed Bi facilitated generation of oxygenated species on the catalyst surface and thus enhanced the inherent activity of the catalyst. The PdCuBi/C catalyst exhibited very high catalytic activity at 171.1 mA cm^{-2} towards ethylene glycol oxidation in alkaline medium. Durability and tolerance towards strongly adsorbed intermediate poisoning of the catalyst were also greatly improved compared to Pd/C. The stability research of PdCuBi/C during a long-term use in fuel cells will be carried out in future. The excellent performance makes the PdCuBi/C catalyst a feasible candidate for the application in alkaline fuel cells.

Acknowledgments

This work was financially supported by the One Hundred Talents Program of the Chinese Academy of Sciences and the Open Fund of Fujian Provincial Key Laboratory of Automotive Electronics and Electric Drive (Fujian University of Technology) (ZDKA1307).

References

[1] K. Matsuoka, M. Inaba, Y. Iriyama, T. Abe, Z. Ogumi, M. Matsuoka, Fuel Cells 2 (2002) 35–39.
[2] E. Peled, V. Livshits, T. Duvdevani, J. Power Sources 106 (2002) 245–248.
[3] V. Livshits, M. Philosoph, E. Peled, J. Power Sources 178 (2008) 687–691.
[4] J.L. Lin, J.R. Ren, N. Tian, Z.Y. Zhou, S.G. Sun, J. Electroanal. Chem. 688 (2013) 165–171.
[5] C. Jin, Y. Song, Z. Chen, Electrochim. Acta 54 (2009) 4136–4140.
[6] P.K. Shen, C. Xu, Electrochem. Commun. 8 (2006) 184–188.
[7] J. Liu, J. Ye, C. Xu, S.P. Jiang, Y. Tong, J. Power Sources 177 (2008) 67–70.
[8] M.H. Shao, T. Huang, P. Liu, J. Zhang, K. Sasaki, M.B. Vukmirovic, R.R. Adzic, Langmuir 22 (2006) 10409–10415.
[9] C. Shen, Y.J. Wang, J.H. Xu, K. Wang, G.S. Luo, Langmuir 28 (2012) 7519–7527.
[10] M. Simões, S. Baranton, C. Coutanceau, Appl. Catal. B Environ. 110 (2011) 40–49.
[11] M. Chen, B. Wu, J. Yang, N. Zheng, Adv. Mater. 24 (2012) 862–879.
[12] K. Tedsree, T. Li, S. Jones, C.W.A. Chan, K.M.K. Yu, P.A.J. Bagot, E.A. Marquis, G.D.W. Smith, S.C.E. Tsang, Nat. Nanotechnol. 6 (2011) 302–307.
[13] H.L. Lu, W.N. Ye, P.Z. Guo, Q.C. Wang, C.J. Lu, X.S. Zhao, Adv. Mater. 709 (2013) 11–14.
[14] J. Cai, Y. Huang, Y. Guo, Electrochim. Acta 99 (2013) 22–29.
[15] C. Hu, H. Cheng, Y. Zhao, Y. Hu, Y. Liu, L. Dai, L. Qu, Adv. Mater. 24 (2012) 5493–5498.
[16] A. Serov, U. Martinez, A. Falase, P. Atanassov, Electrochem. Commun. 22 (2012) 193–196.
[17] R.R. Adžić, N.M. Marković, Electrochim. Acta 30 (1985) 1473–1479.
[18] S. Papadimitriou, S. Armyanov, E. Valova, A. Hubin, O. Steenhaut, E. Pavlidou, G. Kokkinidis, S. Sotiropoulos, J. Phys. Chem. C 114 (2010) 5217–5223.
[19] R.N. Singh, A. Singh, Anindita, Int. J. Hydrogen Energy 34 (2009) 2052–2057.
[20] C.R. Alentejano, I.V. Aoki, Electrochim. Acta 49 (2004) 2779–2785.
[21] A.R. Denton, N.W. Ashcroft, Phys. Rev. A 43 (1991) 3161–3164.
[22] E. Lee, A. Murthy, A. Manthiram, Electrochim. Acta 56 (2011) 1611–1618.
[23] X. Wang, W. Wang, Z. Qi, C. Zhao, H. Ji, Z. Zhang, Int. J. Hydrogen Energy 37 (2012) 2579–2587.
[24] J. Knudsen, A.U. Nilekar, R.T. Vang, J. Schnadt, E.L. Kunkes, J.A. Dumesic, M. Mavrikakis, F. Besenbacher, J. Am. Chem. Soc. 129 (2007) 6485–6490.
[25] P. Mani, R. Srivastava, P. Strasser, J. Phys. Chem. C 112 (2008) 2770–2778.
[26] M. Futamata, L.Q. Luo, J. Power Sources 164 (2007) 532–537.
[27] Y. Huang, J. Cai, Y. Guo, Appl. Catal. B: Environ. 129 (2013) 549–555.